*Advanced Robotics*, Vol. 00, No. 0, pp. 1–18 (2006)

Also available online - www.vsppub.com

*Full paper*

# Haptic interface through wave transformation using delayed reflection: application to a passive haptic device

JAE-HYEONG LEE [1,2,*], CHANG-HYUN CHO [1], MUNSANG KIM [1] and JAE-BOK SONG [2]

[1] *Intelligent Robotics Research Center, Korea Institute of Science and Technology, Hawolgok-dong, Seongbuk-gu, Seoul 136-791, South Korea*
[2] *Department of Mechanical Engineering, Korea University, 5, Anam-dong, Seongbuk-gu, Seoul 136-701, South Korea*

Received 1 March 2005; accepted 14 June 2005

**Abstract**—From the viewpoint of passivity, it is well known that wave variables are robust to transmission delay of a system. During wave transformation for the sampled-data system, a unit delay arises due to causality of the reflection wave. This delay makes the wave transformation in the sampled-data system different from the standard one in the continuous-time system. The unit delay on the reflection wave occasionally becomes a passive element. From the passivity condition of the sampled-data system, the wave impedance can be designed such that wave transformation using delayed reflection provides the effect of positive damping and thus a stable haptic interface is achieved in the sampled-data system. For a passive haptic device, although it is always considered stable because of its passive nature, the oscillatory motion appears during the wall-following task with force approximation. Various experiments for a two-linked passive haptic device show that a stable haptic interface can be accomplished for the wall-following task through wave transformation using delayed reflection.

*Keywords*: Delayed reflection; haptic interface; sampled-data system; wave transformation



## 1. INTRODUCTION

In the conventional haptic interface, since the contact force is constant during one sampling period, the system generates some energy. It is generally known that a haptic interface in the sampled-data system sometimes exhibits unstable behavior, especially when a large amount of power is involved (e.g. a high stiffness wall). A passive actuator such as a brake is stable and has the advantage of a good torque/mass ratio. However, it has a very serious limitation in generating its braking

*To whom correspondence should be addressed. E-mail: quarky@kist.re.kr

torque: passive actuators can generate a torque only against the direction of its motion. Due to this inability of a passive actuator, a desired force can be displayed only approximately in some regions. Moreover, a similar oscillatory motion appears during the wall-following task with force approximation.

The wave transformation or wave variables have been widely used to cope with transmission delay for bilateral teleoperation. Anderson and Spong suggested a delayed transmission line designed for bilateral teleoperation using the passivity and scattering theory. In this transmission line, the norm of the scattering matrix was unity and no loss occurred [1]. Niemeyer and Slotine generalized the study of Anderson and Spong by introducing wave variables. They showed that a transmission delay was not an active element in the wave space described by the wave variables [2]. Wave variables stem from the scattering parameter which is the ratio of the reflected power wave to the incident power wave [3]. Wave variables were mainly used to cope with transmission delays for bilateral teleoperation [4, 5].

Wave transformation has been mostly studied in the continuous-time system. Wave transformation for the sampled-data system inevitably has a unit delay which corresponds to the length of the sampling period of the system. This delay is required for the causality due to the reflection wave, which is the feedback wave used to compute the other wave variable. Therefore, this unit delay makes wave transformation for the sampled-data system different from standard wave transformation in the continuous-time system. Since the wave transformation implemented in the sampled-data system includes the unit delayed reflection wave, this will be referred to as wave transformation using the unit delayed reflection wave or simply *wave transformation using delayed reflection* (WTDR).

In the haptic interface, there are several active elements such as the time delay due to numerical integration and sampling and quantization related to the discrete-time system. Colgate and Schenkel found that an active virtual wall could make the haptic interface unstable, and presented the theoretical passivity condition for the haptic interface implemented on the sampled-data system [6, 7]. In their research, they suggested that an increase in damping of the haptic device and sampling frequency could improve the stability of the haptic interface. Hannaford and Ryu suggested a passivity controller based on the passivity observer in the time domain [8]. Most research on haptic interfaces has focused on designing fixed or varying virtual coupling using power variables such as the force and velocity [9–11].

For systems sensitive to the length of the sampling period such as the haptic interface, this unit delay affects the stability and transparency of the system. From the viewpoint of passivity, the reflection wave including a unit delay can be a passive or active element depending on the choice of the wave impedance. The wave impedance that determines the behavior of a system is an essential parameter in the wave transformation. It is desirable that the wave impedance can be designed such that the unit delayed reflection wave represents a positive damping element.

From the passivity condition of the sampled-data system, it is noted that wave transmission through WTDR is occasionally a passive element (i.e. positive damp-

ing) depending on the choice of the sampling period and wave impedance. This paper provides a guideline for the design of wave impedance that makes the haptic interface stable by considering the passivity condition of a sampled-data system.

Force approximation applied to a passive haptic device is inevitable and is frequently used especially on the wall-following task in which the human operator wants to move the end-effector along the surface of a virtual wall. During the wall-following task, unsmooth motion (i.e. contact and non-contact of the end-effector with a virtual wall) is often observed. Colgate noted that force approximation causes such an unsmooth motion [12]. Furthermore, Colgate and Schenkel found that an active virtual wall could make the haptic interface unstable and presented the theoretical passivity condition for the haptic interface implemented in the sampled-data system [13]. The experiments using a two-linked passive haptic device showed that the haptic interface through the WTDR could produce satisfactory performance for the wall-following task on the virtual environment.

Section 2 introduces the wave variables. Section 3 deals with the basic haptic interface, the fundamental limits of the conventional haptic interface and the condition for the passive interface. The wave transformation and passivity condition for the sampled-data system are discussed in Section 4. In Section 5, the stable haptic interface is extended to a passive haptic system and experimental results are presented. Finally, conclusions are drawn in Section 6.

## 2. WAVE TRANSFORMATION

Power is usually described by power variables such as force and velocity. It can be also represented by wave variables which will be defined below. The wave transformation indicates the conversion between power variables and wave variables. Figure 1 illustrates two types of wave transformation. The configuration of Fig. 1a is called the impedance-type wave transformation because the velocity and force are the input and output of the system, respectively. Likewise, the configuration of Fig. 1b is called the admittance-type wave transformation. It is

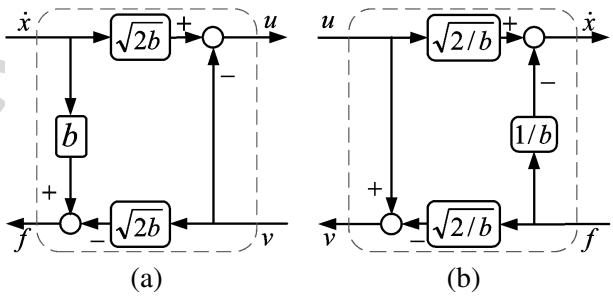


**Figure 1.** Wave transformations. (a) Impedance type. (b) Admittance type.

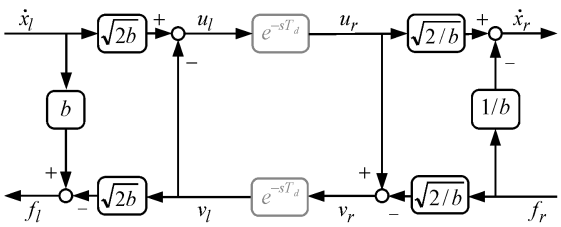


**Figure 2.** Time-delayed transmission through wave transformation.

easily seen that these two types generate the identical relation as follows:

$$\begin{bmatrix} u \\ v \end{bmatrix} = W := GP = \begin{bmatrix} 1/\sqrt{2b} & \sqrt{b/2} \\ -1/\sqrt{2b} & \sqrt{b/2} \end{bmatrix} \begin{bmatrix} f \\ \dot{x} \end{bmatrix}, \tag{1}$$

where $b$ is the wave impedance which determines the behavior of a system, $\dot{x}$ and $f$ are the velocity and force, and $u$ and $v$ are the forward (or incident) and backward (or reflected) waves, respectively. And $G$ represents the transformation matrix, and $W$ and $P$ are the vectors of wave variables and power variables, respectively. Since the wave transformation is one-to-one, the inverse of (1) is uniquely determined as:

$$\begin{bmatrix} f \\ \dot{x} \end{bmatrix} = P := G^{-1}W = \begin{bmatrix} \sqrt{b/2} & -\sqrt{b/2} \\ 1/\sqrt{2b} & 1/\sqrt{2b} \end{bmatrix} \begin{bmatrix} u \\ v \end{bmatrix}. \tag{2}$$

From the viewpoint of passivity, the wave variables are robust to arbitrary time delays [2]. Figure 2 shows a bilateral transmission through the wave transformation that is called the wave transmission. From Fig. 2, the time-delayed transmission can be represented in terms of the input and output vectors:

$$\begin{bmatrix} f_\mathrm{l} \\ -\dot{x}_\mathrm{r} \end{bmatrix} = O(s) := H(s)I(s) = \begin{bmatrix} \dfrac{b(1-\mathrm{e}^{-2sT_\mathrm{d}})}{1+\mathrm{e}^{-2sT_\mathrm{d}}} & \dfrac{2\mathrm{e}^{-sT_\mathrm{d}}}{1+\mathrm{e}^{-2sT_\mathrm{d}}} \\ -\dfrac{2\mathrm{e}^{-sT_\mathrm{d}}}{1+\mathrm{e}^{-2sT_\mathrm{d}}} & \dfrac{1-\mathrm{e}^{-2sT_\mathrm{d}}}{b(1+\mathrm{e}^{-2sT_\mathrm{d}})} \end{bmatrix} \begin{bmatrix} \dot{x}_\mathrm{l} \\ f_\mathrm{r} \end{bmatrix}, \tag{3}$$

where $T_\mathrm{d}$ is the transmission delay, subscripts l and r denote the left and right ports, and $I(s)$, $O(s)$ and $H(s)$ are the input and output vectors and hybrid transformation matrix, respectively. From linear system theory and network theory, the passivity condition of a system whose transfer matrix is $H(s)$ can be written as:

$$H(s) + H^*(s) \geqslant 0, \quad \mathrm{Re}(s) \geqslant 0, \tag{4}$$

where $H^*(s)$ is conjugate transpose matrix of $H(s)$. That is, if a hermitian matrix is positive semi-definite in the right half of the $s$-plane, then the system is passive. From (3), it can be known that the hermitian matrix of $H(s)$ is positive semi-definite. Therefore, the time-delayed transmission through wave transformation is passive. It is well known that a passive system is stable.

Passivity of the delayed transmission line can be verified by computing the overall energy as follows:

$$\int_0^t P_{\text{in}}(\tau)\,\mathrm{d}\tau = E_{\text{stored}}(t) \geqslant 0, \tag{5}$$

where the initially stored energy $E_{\text{stored}}(0)$, the initial condition $P_{\text{in}}(0)$ and power dissipation are zero. From the definition of wave transformation, the power entering a system can be written as

$$P_{\text{in}}(t) = \dot{x}_{\text{l}}^{\text{T}}(t) f_{\text{l}}(t) - \dot{x}_{\text{r}}^{\text{T}}(t) f_{\text{r}}(t), \tag{6}$$

$$P_{\text{in}}(t) = \frac{1}{2}\left\{u_{\text{l}}^{\text{T}}(t)u_{\text{l}}(t) - v_{\text{l}}^{\text{T}}(t)v_{\text{l}}(t) - u_{\text{r}}^{\text{T}}(t)u_{\text{r}}(t) + v_{\text{r}}^{\text{T}}(t)v_{\text{r}}(t)\right\}. \tag{7}$$

Equation (6) can be rewritten by including the transmission delay time $T_{\text{d}}$ as:

$$P_{\text{in}}(t) = \frac{1}{2}\left\{u_{\text{l}}^{\text{T}}(t)u_{\text{l}}(t) - u_{\text{l}}^{\text{T}}(t-T_{\text{d}})u_{\text{l}}(t-T_{\text{d}}) - v_{\text{r}}^{\text{T}}(t-T_{\text{d}})v_{\text{r}}(t-T_{\text{d}}) + v_{\text{r}}^{\text{T}}(t)v_{\text{r}}(t)\right\}, \tag{8}$$

where $u_{\text{r}}(t) = u_{\text{l}}(t - T_{\text{d}})$ and $v_{\text{l}}(t) = v_{\text{r}}(t - T_{\text{d}})$. Passivity can be checked by integrating $P_{\text{in}}(t)$. From (5) and (8), the passivity condition of the delayed transmission line can be written as:

$$E_{\text{stored}}(t) = \frac{1}{2}\int_{t-T_{\text{d}}}^{t} \left\{u_{\text{l}}^{\text{T}}(\tau)u_{\text{l}}(\tau) + v_{\text{r}}^{\text{T}}(\tau)v_{\text{r}}(\tau)\right\}\mathrm{d}\tau \geqslant 0. \tag{9}$$

Therefore, the delayed transmission line is passive. This result is the same as that of (4), but the time delay should be constant.

## 3. BASIC HAPTIC INTERFACE

### *3.1. Definition*

Figure 3 illustrates a simple haptic interface in which the haptic device and virtual environment are modeled by the mass $m_{\text{d}}$ and the spring $k_{\text{ve}}$, respectively. The haptic device is moved by the human force $f_{\text{h}}$. When the device is in contact with the virtual environment, the reaction force $f_{\text{ve}}$ can be computed as the product of the spring stiffness, $k_{\text{ve}}$, and the displacement of the virtual spring, $x_{\text{ve}}$. This reaction force is transmitted to the operator through the haptic device, supposing that there is

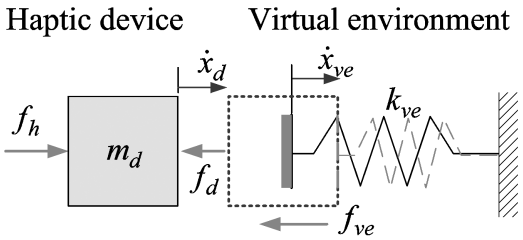


**Figure 3.** Basic haptic interface.

no transmission delay. The dynamics of the haptic device and virtual environment can be written as:

$$m_{\mathrm{d}}\frac{\mathrm{d}}{\mathrm{d}t}\dot{x}_{\mathrm{d}}(t) = f_{\mathrm{h}}(t) - f_{\mathrm{d}}(t), \tag{10}$$

$$k_{\mathrm{ve}}\int_0^t \dot{x}_{\mathrm{ve}}(\tau)\,\mathrm{d}\tau = f_{\mathrm{ve}}(t), \tag{11}$$

where $f_{\mathrm{d}}$ is the transmitted force from the virtual environment to the haptic device, and $\dot{x}_{\mathrm{d}}$ and $\dot{x}_{\mathrm{ve}}$ are the velocities of the haptic device and virtual environment, respectively. In the case of the haptic device in contact with the virtual environment, $\dot{x}_{\mathrm{d}} = \dot{x}_{\mathrm{ve}}$ and $f_{\mathrm{d}} = f_{\mathrm{ve}}$. Therefore, the dynamics of the haptic interface can be represented as:

$$m_{\mathrm{d}}\frac{\mathrm{d}}{\mathrm{d}t}\dot{x}_{\mathrm{ve}}(t) + k_{\mathrm{ve}}\int_0^t \dot{x}_{\mathrm{ve}}(\tau)\,\mathrm{d}\tau = f_{\mathrm{h}}(t). \tag{12}$$

Equation (12) is a simple mass–spring system. It is generally known that the ideal haptic interface based on (12) is passive and lossless.

### 3.2. Active wall

In practice, the virtual environment cannot be composed of only linear components. The basic haptic interface of Fig. 3 can be implemented in Fig. 4 using non-linear elements such as a sampler, ZOH and unilateral constraint. In Fig. 4, the asterisk denotes the discrete-time signal.

The passivity of the sampled-data system can be given by:

$$b_{\mathrm{d}} > \frac{T_{\mathrm{s}}}{2}(1-\cos\omega T_{\mathrm{s}})^{-1}\mathrm{Re}\left\{(1-\mathrm{e}^{-j\omega T_{\mathrm{s}}})H_{\mathrm{ve}}(\mathrm{e}^{j\omega T_{\mathrm{s}}})\right\}, \tag{13}$$

where $s = j\omega$, $T_{\mathrm{s}}$ is the sampling period of the system, $b_{\mathrm{d}}$ is the viscous damping of the haptic device and $H_{\mathrm{ve}}(\mathrm{e}^{j\omega T})$ is the discrete transfer function of the virtual environment [7]. Equation (13) compares the magnitude of viscous damping of the haptic device with the real part of the result from computing the virtual environment on the sample-data system. As an example, when (13) is applied to the system of

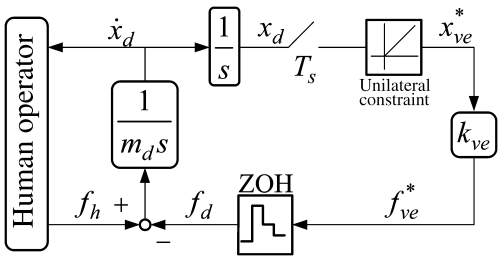


**Figure 4.** Basic haptic interface in the sampled-data system.

Fig. 4, the passivity condition can be written as:

$$0 > \frac{T_s}{2}(1-\cos\omega T_s)^{-1}\mathrm{Re}\left\{(1-\mathrm{e}^{-j\omega T_s})k_{ve}\right\} = \frac{k_{ve}T_s}{2}, \tag{14}$$

where, since $b_d = 0$, the system is passive if and only if $k_{ve}T_s < 0$, but it is impossible to satisfy this condition, since $k_{ve} > 0$ and $T_s > 0$. Hence, the system is intrinsically active.

It is well known that a virtual wall can become active, while a real physical wall is always passive. Figure 5 illustrates the active nature of a virtual wall by investigating the contact of the haptic device with the virtual wall shown in Fig. 4, in which very unstable behavior of the haptic system is observed. Suppose the haptic device initially at 0 mm deformed the wall at 0.01 m by the haptic device driven by the hand force. During this operation, the virtual wall modeled as a virtual spring generated energy, thus serving as an active element. The stiffness of the virtual wall $k_{ve}$, sampling frequency $T_s$ and hand force $f_h$ are 5 kN/m, 10 kHz and 3 N, respectively. This harder contact caused the unstable behavior, thus leading to the highly oscillatory response and negative energy showing the active nature of the haptic device.

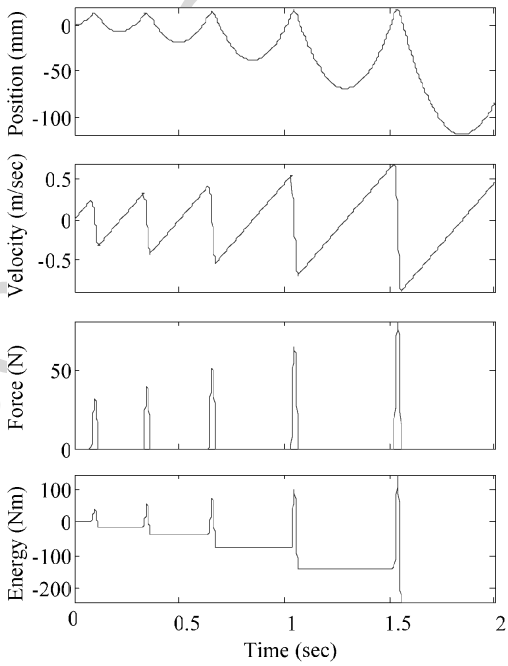


**Figure 5.** Example of a basic haptic interface ($k_{ve} = 10$ kN/m, $T_s = 1$ ms, $m_d = 1$ kg and $f_h = 3$ N).

## 4. WAVE TRANSFORMATION USING DELAYED REFLECTION

### 4.1. Wave transformation in sampled-data system

As illustrated in Figs 2 and 6, one wave variable $u$ (or $v$) depends on the information of the other wave variable $v$ (or $u$), which is called the *reflection wave*. When wave transformations are conducted in the continuous-time system, wave variables can respond immediately to their reflection waves. In the sampled-data (or discrete-time) system, however, variables cannot respond immediately, but a time delay $T_s$, which corresponds to the sampling period of the system, is inevitably introduced. Moreover, according to the choice of the signal flow, the unit delay can be placed at other places. As shown Fig. 4, if the signal flows have two loops and each loop simultaneously starts from computing each wave variables, the unit delay is placed at the reflection wave. Then, in computing $u_l(t)$, $v_l(t - T_s)$ is used in place of $v_l(t)$. The factor $v_l(t - T_s)$ or $u_r(t - T_s)$ is called a reflection wave with unit delay or *delayed reflection*.

Another choice, e.g. the unit delay for the admittance type, is placed between $\dot{x}_r$ and $f_r$ so that $(1/b)e^{-sT_s}$ is used instead of $1/b$. In this paper, the wave transformation in the sampled-data system is restricted to WTDR in which a unit delay is associated with reflection wave variables, not power variables.

The WTDR can be written as:

$$\begin{bmatrix} u_l \\ v_l \end{bmatrix} = W_l := G_I P_l = \begin{bmatrix} e^{-sT_s}/\sqrt{2b} & (2 - e^{-sT_s})\sqrt{b/2} \\ -1/\sqrt{2b} & \sqrt{b/2} \end{bmatrix} \begin{bmatrix} f_l \\ \dot{x}_l \end{bmatrix}, \tag{15}$$

$$\begin{bmatrix} u_r \\ v_r \end{bmatrix} = W_r := G_A P_r = \begin{bmatrix} 1/\sqrt{2b} & \sqrt{b/2} \\ -(2 - e^{-sT_s})/\sqrt{2b} & e^{-sT_s}\sqrt{b/2} \end{bmatrix} \begin{bmatrix} f_r \\ \dot{x}_r \end{bmatrix}, \tag{16}$$

where the subscripts I and A denote the impedance and admittance types, respectively. The inverses of (15) and (16) are unique as:

$$G_I^{-1} = \begin{bmatrix} \sqrt{b/2} & -(2 - e^{-sT_s})\sqrt{b/2} \\ 1/\sqrt{2b} & e^{-sT_s}/\sqrt{2b} \end{bmatrix}, \tag{17}$$

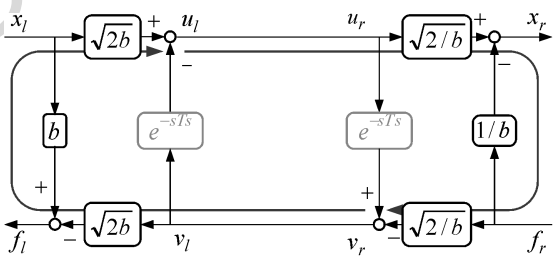


**Figure 6.** Wave transmission through the WTDR.

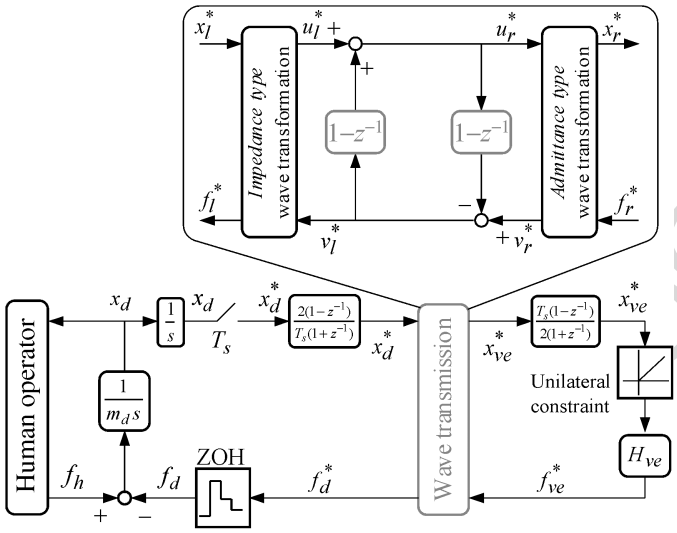


**Figure 7.** Basic haptic interface through the WTDR.

$$G_{\mathrm{A}}^{-1} = \begin{bmatrix} \mathrm{e}^{-sT_{\mathrm{s}}}\sqrt{b/2} & -\sqrt{b/2} \\ (2-\mathrm{e}^{-sT_{\mathrm{s}}})/\sqrt{2b} & 1/\sqrt{2b} \end{bmatrix}. \tag{18}$$

Since $W_{\mathrm{l}} = W_{\mathrm{r}}$ in Fig. 7, we get:

$$G_{\mathrm{I}} P_{\mathrm{l}} = G_{\mathrm{A}} P_{\mathrm{r}}. \tag{19}$$

Thus:

$$P_{\mathrm{l}} = G_{\mathrm{I}}^{-1} G_{\mathrm{A}} P_{\mathrm{r}}. \tag{20}$$

From (15) and (18), we get:

$$\begin{bmatrix} f_{\mathrm{l}} \\ \dot{x}_{\mathrm{l}} \end{bmatrix} = \frac{1}{2} \begin{bmatrix} 1+(2-\mathrm{e}^{-sT_{\mathrm{s}}})^2 & b(1-\mathrm{e}^{-sT_{\mathrm{s}}})^2 \\ (1-\mathrm{e}^{-sT_{\mathrm{s}}})^2/b & 1+\mathrm{e}^{-2sT_{\mathrm{s}}} \end{bmatrix} \begin{bmatrix} f_{\mathrm{r}} \\ \dot{x}_{\mathrm{r}} \end{bmatrix}. \tag{21}$$

Rearrangement of (21) yields the following input–output relation of wave variables:

$$\begin{bmatrix} f_{\mathrm{l}} \\ -\dot{x}_{\mathrm{r}} \end{bmatrix} = \begin{bmatrix} \dfrac{b(1-\mathrm{e}^{-sT_{\mathrm{s}}})^2}{1+\mathrm{e}^{-2sT_{\mathrm{s}}}} & \dfrac{2}{1+\mathrm{e}^{-2sT_{\mathrm{s}}}} \\ -\dfrac{2}{1+\mathrm{e}^{-2sT_{\mathrm{s}}}} & \dfrac{(1-\mathrm{e}^{-sT_{\mathrm{s}}})^2}{b(1+\mathrm{e}^{-2sT_{\mathrm{s}}})} \end{bmatrix} \begin{bmatrix} \dot{x}_{\mathrm{l}} \\ f_{\mathrm{r}} \end{bmatrix}. \tag{22}$$

### *4.2. Passivity condition for the WTDR*

When the WTDR is applied to the basic haptic interface, the whole system can be represented in Fig. 7. From Fig. 7, the velocity and force of the virtual environment

have the relation:

$$f_{\mathrm{ve}}^* = k_{\mathrm{ve}} \frac{T_{\mathrm{s}}(1 - \mathrm{e}^{-sT_{\mathrm{s}}})}{2(1 + \mathrm{e}^{-sT_{\mathrm{s}}})} \dot{x}_{\mathrm{ve}}^*, \tag{23}$$

where $z = \mathrm{e}^{sT_{\mathrm{s}}}$. From (21), the relation of the power variables between the haptic device and the virtual environment can be written as follows:

$$\begin{bmatrix} f_{\mathrm{d}}^* \\ \dot{x}_{\mathrm{d}}^* \end{bmatrix} = \frac{1}{2} \begin{bmatrix} 1 + (2 - \mathrm{e}^{-sT_{\mathrm{s}}})^2 & b(1 - \mathrm{e}^{-sT_{\mathrm{s}}})^2 \\ (1 - \mathrm{e}^{-sT_{\mathrm{s}}})^2 / b & 1 + \mathrm{e}^{-2sT_{\mathrm{s}}} \end{bmatrix} \begin{bmatrix} f_{\mathrm{ve}}^* \\ \dot{x}_{\mathrm{ve}}^* \end{bmatrix}. \tag{24}$$

Suppose that the component exempt for the haptic device and the connection component for the discrete system (e.g. sampler and ZOH) are the virtual environments. Combining (23) and (24), the transfer function of the virtual environment which includes the wave transformation can be obtained (without the unilateral constraint) by:

$$H_{\mathrm{ve}}(\mathrm{e}^{sT_{\mathrm{s}}}) = \frac{4b^2(1 - \mathrm{e}^{-sT_{\mathrm{s}}})^4 + 4bk_{\mathrm{ve}}T_{\mathrm{s}}(1 - \mathrm{e}^{-2sT_{\mathrm{s}}})\{1 + (2 - \mathrm{e}^{-sT_{\mathrm{s}}})^2\}}{2bT_{\mathrm{s}}(1 - \mathrm{e}^{-4sT_{\mathrm{s}}}) + k_{\mathrm{ve}}T_{\mathrm{s}}^2(1 - \mathrm{e}^{-2sT_{\mathrm{s}}})^2}, \tag{25}$$

where $H_{\mathrm{ve}} = f_{\mathrm{d}}^*/x_{\mathrm{d}}^*$. To verify the passivity of the system, applying the transfer function (25) to the passivity condition of (13) gives:

$$Q(b, \omega) = \frac{2(k_{\mathrm{ve}}T_{\mathrm{s}} - 2b)(k_{\mathrm{ve}}T_{\mathrm{s}} + (k_{\mathrm{ve}}T_{\mathrm{s}} - 2b)\cos(\omega T_{\mathrm{s}}))}{4b^2 + k_{\mathrm{ve}}^2T_{\mathrm{s}}^2 + (4b^2 - k_{\mathrm{ve}}^2T_{\mathrm{s}}^2)\cos(2\omega T_{\mathrm{s}})} - 1 < 0, \tag{26}$$

where $0 \leqslant \omega \leqslant \pi/T_{\mathrm{s}}$. The critical points of the function $Q(b, \omega)$ can be found for the boundary values and the values satisfying $\partial Q/\partial\omega = 0$ as follows:

$$\frac{k_{\mathrm{ve}}T_{\mathrm{s}}(k_{\mathrm{ve}}T_{\mathrm{s}} - 3b)}{2b^2}, \tag{27a}$$

$$\frac{4b^2 - 8bk_{\mathrm{ve}}T_{\mathrm{s}} - k_{\mathrm{ve}}^2T_{\mathrm{s}}^2 - 4k_{\mathrm{ve}}T_{\mathrm{s}}\sqrt{b(2b + k_{\mathrm{ve}}T_{\mathrm{s}})}}{2k_{\mathrm{ve}}T_{\mathrm{s}}(2b + k_{\mathrm{ve}}T_{\mathrm{s}}) + 4k_{\mathrm{ve}}T_{\mathrm{s}}\sqrt{b(2b + k_{\mathrm{ve}}T_{\mathrm{s}})}}, \tag{27b}$$

$$\frac{4b^2 - 8bK_{\mathrm{ve}}T_{\mathrm{s}} - k_{\mathrm{ve}}^2T_{\mathrm{s}}^2 + 4k_{\mathrm{ve}}T_{\mathrm{s}}\sqrt{b(2b + k_{\mathrm{ve}}T_{\mathrm{s}})}}{2k_{\mathrm{ve}}T_{\mathrm{s}}(2b + k_{\mathrm{ve}}T_{\mathrm{s}}) - 4k_{\mathrm{ve}}T_{\mathrm{s}}\sqrt{b(2b + k_{\mathrm{ve}}T_{\mathrm{s}})}}, \tag{27c}$$

$$\frac{k_{\mathrm{ve}}T_{\mathrm{s}} - 4b}{2b}. \tag{27d}$$

From the critical points, the maximum values of the function $Q(b, \omega)$ are:

$$\frac{k_{\mathrm{ve}}T_{\mathrm{s}}(k_{\mathrm{ve}}T_{\mathrm{s}} - 3b)}{2b^2} \quad \text{where } 2b < k_{\mathrm{ve}}T_{\mathrm{s}}, \tag{28a}$$

$$\frac{4b^2 - 8bk_{\mathrm{ve}}T_{\mathrm{s}} - k_{\mathrm{ve}}^2T_{\mathrm{s}}^2 - 4k_{\mathrm{ve}}T_{\mathrm{s}}\sqrt{b(2b + k_{\mathrm{ve}}T_{\mathrm{s}})}}{2k_{\mathrm{ve}}T_{\mathrm{s}}(2b + k_{\mathrm{ve}}T_{\mathrm{s}}) + 4k_{\mathrm{ve}}T_{\mathrm{s}}\sqrt{b(2b + k_{\mathrm{ve}}T_{\mathrm{s}})}} \quad \text{where } 2b > k_{\mathrm{ve}}T_{\mathrm{s}}. \tag{28b}$$

If the maximum value of $Q(b, \omega)$ is less than zero, the haptic interface through the WTDR is passive. From (28), the maximum value of $Q(b, \omega)$ is less than zero

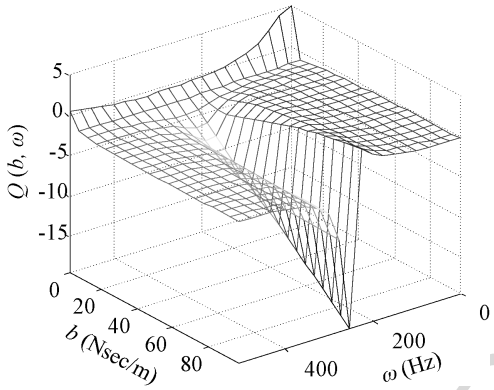


**Figure 8.** $Q(b, \omega)$ as a function of frequency and wave impedance.

over the entire frequency range where:

$$0.333 < b/(k_{\text{ve}} T_{\text{s}}) < 3.579. \tag{29}$$

Figure 8 shows the graph for $Q(b, \omega)$ over frequency with $k_{\text{ve}} = 10$ kN/m and $T_{\text{s}} = 1$ ms.

If the passivity condition is applied to the system of Fig. 7, the haptic interface becomes passive as shown in Fig. 9. The parameters used in this simulation are the same as those of Fig. 5. From (29) and the value of $k_{\text{ve}} T_{\text{s}}$, the wave impedance used in the simulation was set to 35 Ns/m.

It follows from the simulation results that the WTDR with the appropriate wave impedance can make the haptic interface stable. The position, velocity and force responses in Fig. 9 indicate the stable behavior of the haptic interface. Note that the stored energy is kept positive at all times. In the steady state, the wave variables had the same magnitude, but the opposite sign. Their magnitude was $0.118\sqrt{\text{Nm/s}}$. Figure 9b depicts the simulation results that include the transmission delay of 10 ms. When there was the transmission delay, the haptic interface was also stable. However, there occurred a position error between the haptic device and the virtual environment. Furthermore, the settling time was larger than that of the simulation without any transmission delay.

## 5. EXPERIMENT FOR THE PASSIVE HAPTIC DEVICE

In the previous section it was shown that the haptic interface using wave variables can be intrinsically passive depending on the choice of the wave impedance. In the haptic interface, the only difference between the passive and the active haptic device is where to employ the force approximation in the haptic controller for the passive haptic device. Through the passive force manipulability ellipsoid (FME) analysis [14], pullback motion can be analyzed, in which the end-effector can be brought back to the wall surface once it penetrates into the wall. However, the

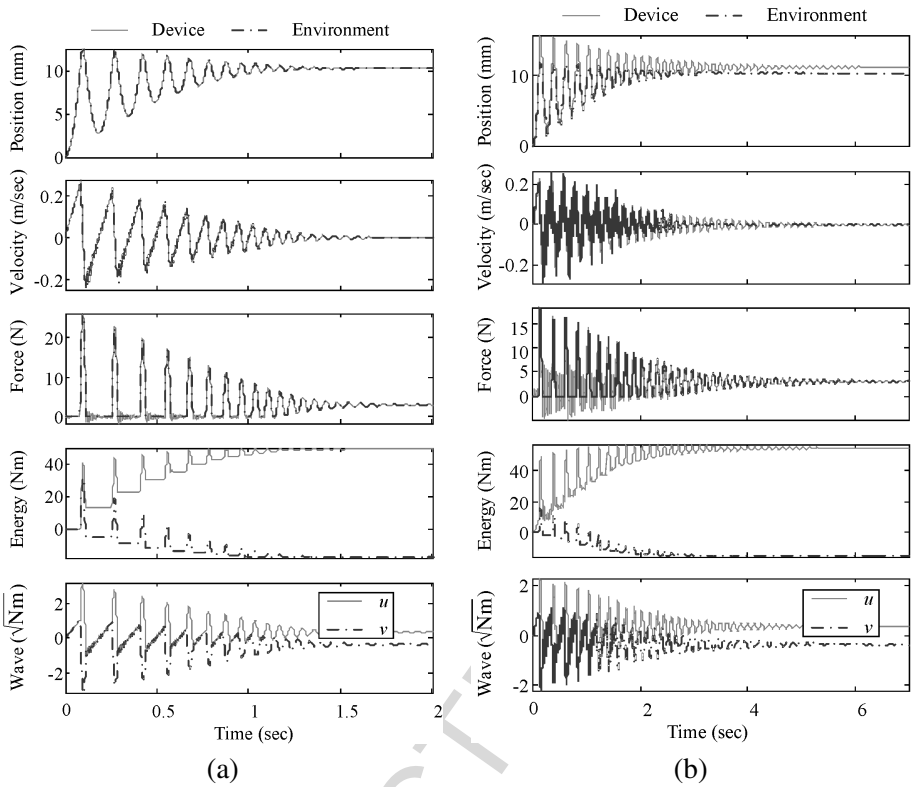


**Figure 9.** Simulation results ($k_{ve} = 10$ kN/m, $T_s = 1$ ms, $m_d = 1$ kg and $f_h = 3$ N, $b = 35$ Nsc/m). (a) Without transmission delay. (b) With transmission delay $T_d = 10$ ms.

force approximation makes the pullback motion partially available for the passive haptic device. A haptic system using the passive haptic device exhibits unstable behavior such as unsmooth motion when it has the pullback capability due to the force approximation as shown Fig. 11 (see later). To obtain a stable haptic interface, the proposed haptic interface in Fig. 7 is applied to the haptic system using the passive haptic device.

The two-link passive haptic device equipped with two electric brakes shown in Fig. 10 was constructed for experiments. The angles $\theta_i$ and $\theta_{Bi}$ represent the joint angle and the rotating angle of the brake, respectively, and $k_i$ is the reduction ratio of the tendon-drive system. The design parameters are $k_2 = 0.4$ and $l_1 = l_2 = 0.15$ m. Brake 1 (or 2) that provides a braking torque to link 1 (or 2) is mounted at the base and conveys the torque through pulleys $P_{1a}$–$P_{1b}$ (or $P_{2a}$–$P_{2b}$). In this situation, $\theta_2$ is computed by:

$$\theta_2 = k_2\theta_{B2} - k_2\theta_1. \tag{30}$$

Note that $\theta_2$ is a function of $\theta_1$ as well as $\theta_{B2}$, i.e. the coupled motion [15] in the wire transmission is observed in $\theta_2$. Placing both brakes at the base has the

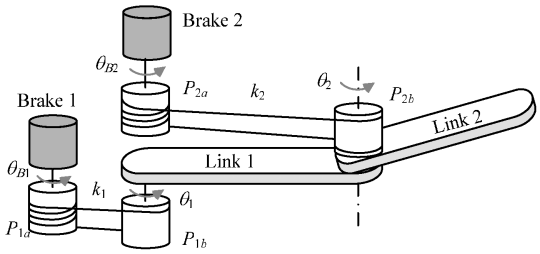


(a)

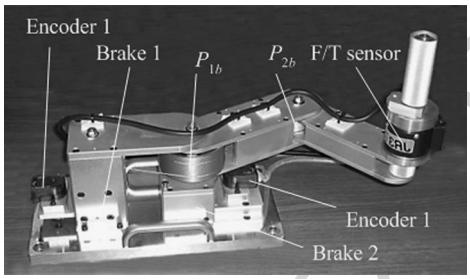


(b)

**Figure 10.** Coupled tendon-drive mechanism. (a) Schematic. (b) Picture.

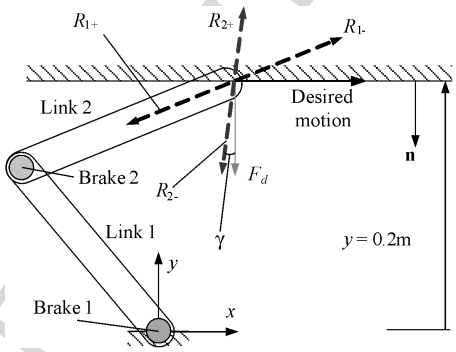


**Figure 11.** Location of the virtual wall and experimental conditions.

advantage of reducing the mass of the moving part. Rotational motion of each brake is sensed by the optical encoder mounted on the brake axis.

A brake can generate its braking torque only in the passive region in which $\tau \cdot \dot{q} \leqslant 0$ is satisfied, where $\dot{q}$ and $\tau$ are the joint velocity and joint torque, respectively. Let $J$ be the Jacobian matrix and $J_i$ be the $i$th column vector of $J^{-\mathrm{T}} = [J_1 \cdots J_n]$. From $F = J(q)^{-\mathrm{T}}\tau$, we can obtain available forces corresponding to joint conditions (e.g. $\dot{q}_i$) by adopting Karnopp's stick–slip model [16] as follows:

$$R_i = -\mathrm{sgn}(\dot{\theta}_i)J_i, \quad \dot{\theta}_i \neq 0 \quad \text{(slip mode)}, \tag{31a}$$

$$R_i = -\mathrm{sgn}(\tau_{\mathrm{h}i})J_i, \quad \dot{\theta}_i = 0 \quad \text{(stick mode)}, \tag{31b}$$

where the subscript $i$ denotes the joint number and $\tau_{hi}$ represents the hand torque input. In this paper $R_i$ is termed the reference force.

Figure 11 shows the experimental conditions. Two brakes generated a braking torque in proportion to the input current at a rate of 1 kHz. The plane virtual wall located at $y = 0.2$ m was modeled as a spring whose spring constant was 10 kN/m, but it was assumed to possess neither damping nor friction on the surface. The wave impedance was set to 35 Nm/s. The experimental conditions were the same as in the numerical simulations except for the use of the passive haptic device. A hand force input was provided to move the handle mounted at the end-effector in the $+x$ direction while it maintained contact with the virtual wall. In order to accomplish this wall-following task, the haptic device is required to display the desired force $F_d$ normal to the virtual surface. However, since the brake can generate a torque only against its rotation or against the externally applied torque, even a combination of two brake torques cannot accurately display this force in this case, which can be easily detected from FME analysis. Hence, the reaction force $F_d$ can be displayed approximately at most by $R_{2-}$ which was obtained with brake 2 activated and brake 1 fully released.

Figure 12 shows the experimental result for the conventional interface which only used the force approximation method without transmission delay. The results show that unsmooth motion (i.e. contact and non-contact) is repeated in the position,

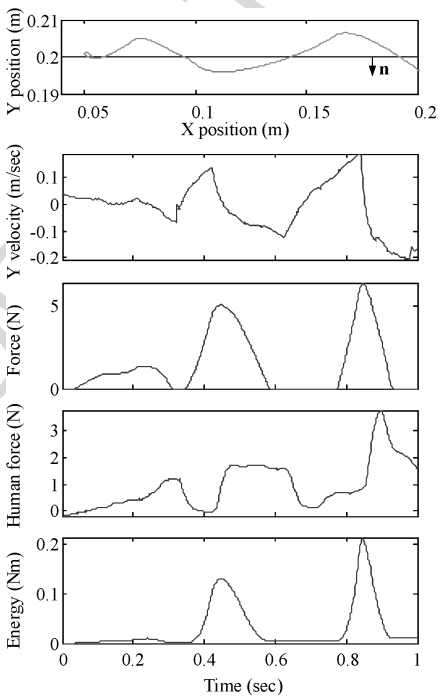


**Figure 12.** Experimental results using the conventional haptic interface ($T_s = 1$ ms, $k_{ve} = 10$ kN/m).

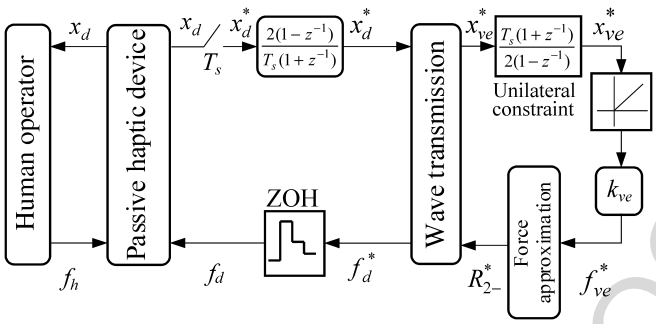


**Figure 13.** Passive haptic interface through wave transformation.

velocity, force and human force. When the device moved from contact to non-contact, the stored energy was positive. Since the passive actuators can inevitably display a desired force by approximation, the passive device absorbs some energy from the active wall. Therefore, the resulting stored energy of the haptic device remained positive. However, from the experimental results, it can be seen that the stored energy was not enough to overcome the active wall.

Figure 13 shows the schematic of the signal flows of the passive haptic interface through wave transformation. The haptic device velocity and the force from the virtual environment were transmitted through wave transformation, which is the only difference from the conventional interface based on a passive haptic device. In the experiment results shown in Fig. 14, smooth paths of the end-effector were observed after the first contact with the virtual wall for the proposed haptic interface. The penetration depth also remained at a relatively constant value. It was shown that the $y$ velocity stayed around zero after contacting the wall. Furthermore, no sudden change that frequently occurred at the conventional interface was observed on the curve of the desired force.

The energy of the system is worth discussing. When the device moved to non-contact, the stored energy remained positive with an amount of the magnitude for the proposed haptic interface. Since the stored energy is greater than that from the active wall, one can obtain the results of Fig. 14. It is noted that the wave variables of the ideal display will remain at a constant value after the initial contact, since there is no sudden change of the device velocity and the environment force. It is also observed in Fig. 14 that the wave variables had the same magnitudes, but the opposite sign, at the steady state, which indicated that the haptic interface was stable.

## 6. CONCLUSIONS

In this paper, wave transformation has been adopted to implement a haptic interface with a passive haptic device, in which the reflection wave variable inevitably includes a unit delay coincident with the sampling period in sampled-data system. From this research, the following conclusions are drawn:

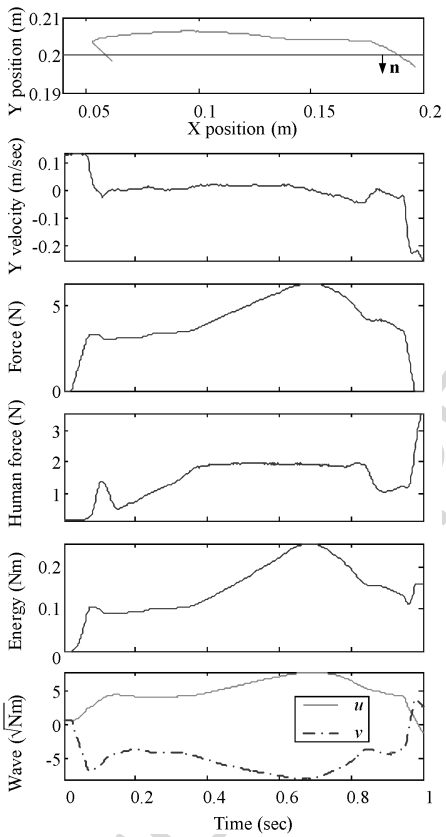


**Figure 14.** Experimental results using the wave transformation ($T_s = 1$ ms, $k_{ve} = 10$ kN/m and $b = 35$ Ns/m).

(i) The wave transmission through *WTDR* can be either an active or a passive element depending on the sampling period and the wave impedance. Its property can be verified with the passivity condition of the sampled-data system. With this property, the haptic can be made stable without additional physical damping.

(ii) The experiments for the passive haptic device also show that a stable haptic interface (smooth wall-following) can be accomplished using the wave transformation. Therefore, the wave transformation is beneficial not only to bilateral teleoperation with time delay, but also to the haptic interface implemented in the sampled-data form.

As a result, it is shown that the wave transmission through WTDR is intrinsically a control method in the haptic interface. Furthermore, the wave transmission through WTDR can serve as a controller for the force-controlled system.

## REFERENCES

1. R. J. Anderson and M. W. Spong, Bilateral control of teleoperators with time delay, *IEEE Trans. Automatic Control* **34**, 494–501 (1989).
2. G. Niemeyer and J. J. Slotine, Stable adaptive teleoperation, *IEEE J. Oceanogr. Eng.* **16**, 152–162 (1991).
3. S. S. Haykin, *Active Netwok Theory.* Addison-Wesley, Reading, MA (1970).
4. S. Munir and W. J. Book, Internet-based teleoperation using wave variables with prediction, *IEEE/ASME Trans. Mechatron.* **7**, 124–133 (2002).
5. Y. Yokokohji, T. Imaida and T. Yoshikawa, Bilateral teleoperation under time-varying communication delay, in: Proc. *IEEE/RSJ Int. Conf. on Intelligent Robots and Systems*, Kyongju, pp. 1854–1859 (1999).
6. J. E. Colgate, P. E. Grafing, M. C. Stanley and G. Schenkel, Implementation of stiff virtual walls in force–reflecting interfaces, in: Proc. *IEEE Virtual Reality Annu. Int. Symp.*, pp. 202–208 (1993).
7. J. E. Colgate and G. G. Schenkel, Passivity of a class of sampled-data systems: application to haptic interface, *J. Robotic Syst.* **14**, 37–47 (1997).
8. B. Hannaford and J.-H. Ryu, Time-domain passivity control of haptic interface, *IEEE Trans. Robotics Automat.* **18**, 1–10 (1999).
9. R. Daniel and P. McAree, Fundamental limits of performance for force reflecting teleoperation, *Int. J. Robotics Res.* **7**, 811–830 (1998).
10. R. J. Adams and B. Hannaford, Stable haptic interface with virtual environment, *Int. J. Robotics Res.* **17**, 811–830 (1999).
11. S. E. Salcudean, M. Zhu, W.-H. Zhu and K. Hashtrudi-Zaad, Transparent bilateral teleoperation under position and rate control, *IEEE Trans. Robotics Automat.* **15**, 465–474 (2000).
12. J. E. Colgate, M. A. Peshkin and W. Wannasuphoprasit, Nonholonomic haptic display, in: *Proc. IEEE Int. Conf. on Robotics and Automation*, pp. 539–544 (1996).
13. J. E. Colgate, P. E. Grafing, M. C. Stanley and G. Schenkel, Implementation of stiff virtual walls in force-reflecting interfaces, in: *Proc. IEEE Virtual Reality Annu. Int. Symp.*, pp. 202–208 (1993).
14. C.-H. Cho, J.-B. Song, M. Kim and C.-S. Hwang, Energy-based control of a passive haptic device, in: *Proc. IEEE Int. Conf. on Robotics and Automation*, pp. 292–297 (2004).
15. S. Ma, H. Yoshinada and S. Hirose, CT ARM-I: coupled tendon-driven manipulator model I — design and basic experiments, *IEEE Trans. Robotics Automat.* 2094–2100 (1992).
16. D. Karnopp, Computer simulation of stick–slip friction in mechanical dynamic system, *ASME J. Dyn. Syst. Meas. Control* **107**, 100–103 (1985).



## ABOUT THE AUTHORS

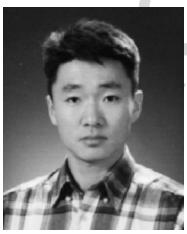

**Jae-Hyeong Lee** received his BS in Physics and MS in Mechanical Engineering from Sogang University, Korea, in 1997 and 1999, respectively, and his PhD degree in Mechanical Engineering from Korea University, Korea, in 2005. Since 1999 he has been working as a Research Scientist at KIST. His current research interests are the design and control of robotic systems including bilateral teleoperation and the haptic devices, and the design and control of trailer systems.

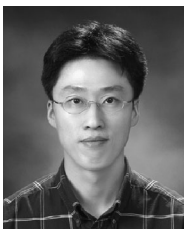

**Chang-Huyn Cho** received his BS and MS in Mechanical Engineering from Kyunghee University, Korea, in 1997 and 1999, respectively, and his PhD degree in Mechanical Engineering from Korea University, Korea, in 2005. He joined the Center for Intelligent Robotics, Frontier 21 Program at KIST in 2005. His current research interests are mechanism design and control of robotic systems.

**Munsang Kim** received his BS and MS in Mechanical Engineering from Seoul National University in 1980 and 1982, respectively, and the DIng in Robotics from the Technical University of Berlin, Germany in 1987. Since 1987, he has been working as a Research Scientist at KIST. He has led the Advanced Robotics Research Center since 2000 and became the Director of the 'Intelligent Robot — The Frontier 21 Program' since October 2003. His current research interests are the design and control of novel mobile manipulation systems, haptic device design and control, and sensor applications to intelligent robots.

**Jae-Bok Song** received his BS and MS in Mechanical Engineering from Seoul National University, Korea, in 1983 and 1985, respectively, and his PhD in Mechanical Engineering from MIT in 1992. He joined the faculty of the Department of Mechanical Engineering, Korea University in 1993, where he has been a Full Professor since 2002. His current research interests are robot navigation, and the design and control of robotic systems including haptic devices.